Modeling of multi-electrode tapered quantum-dot superluminescent diodes

Adam F. Forrest
Institute of Photonics and
Quantum Sciences
Heriot Watt University
Edinburgh, UK
adam.forrest@hw.ac.uk

Maria Ana Cataluna
Institute of Photonics and
Quantum Sciences
Heriot Watt University
Edinburgh, UK
m.cataluna@hw.ac.uk

Michel Krakowski
III-V Lab,
Campus de Polytechnique
Palaiseau, France
michel.krakowski@3-5lab.fr

Paolo Bardella
Dipartimento di Elettronica
e Telecomunicazioni,
Politecnico di Torino,
Turin, Italy
paolo.bardella@polito.it

Abstract—We introduce a rate equation based numerical model suitable for the description of the wide spectral asymmetry experimentally observed at the two facets of multi-electrode tapered superluminescent diode based on Quantum Dot material. Numerical simulations carried out with this model were able to quantitatively reproduce the behavior of a two-section SLD and explain the reported spectral asymmetry in terms of non-uniform filling of the QD confined states under non-uniform current injection.

Keywords—Superluminescent diode, Quantum Dot, Tapered waveguide, spectral asymmetry.

I. Introduction

In this work we propose a model suitable for the description of the spectral properties of the optical emission in multi-electrode superluminescent diodes (SLDs) with tapered a waveguide, based on multi-layer Quantum Dot (QD) material with a chirped composition. This model, validated through a comparison against experimental measurements of an SLD emitting around 1250 nm, provides important insight for the design of these sources, which are attractive for numerous applications, such as optical coherence tomography [1] and high-speed spectroscopy [2] due to their high output powers and large spectral bandwidths.

II. Model Description

The model describes the spectral distribution of the photons (S) in the device longitudinal direction (z), in stationary conditions and extends the model presented in [3,4]. We divide the portion of interest of the optical spectrum into M uniformly distributed intervals with amplitude $2\Delta E$, centered around E_m, so that $S_m^\pm(z)$ ($m \in [1, M]$) indicate the number of photons with energy in the range ($E_m \pm \Delta E/2$) propagating in the forward ($+z$) and backward ($-z$) directions. The spatial evolution of $S_m^\pm(z)$ can be obtained by integrating the differential equations

$$\pm \frac{dS_m^\pm(z)}{dz} = R_m^{sp}(z) + \left(\Gamma^\pm(z)g_m(z) - \alpha_i^\pm - \alpha_p(z)\right)S_m^\pm(z) \quad (1)$$

where $\Gamma^\pm(z)$ and $\alpha_i^\pm$ are direction dependent transverse confinement factor and material losses respectively, which can be extracted from Beam Propagation Method simulations to properly describe weakly guiding waveguides, and $\alpha_p(z)$ are plasma induced losses. The terms $R_m^{sp}(z)$ and $g_m(z)$ model spontaneous emission and the material gain per unit length in the considered energy interval, respectively, and depend on the spontaneous emission $R_{sp}^l(z, E)$ and gain $g^l(z, E)$ of each confined state of each QD layer l of the chirped material. While SLDs are typically anti-reflection coated and tilted to reduce back reflections, we include the boundary conditions $S_m^+(0) = R_0 S_m^-(0)$ and $S_m^-(L) = R_L S_m^+(L)$, with R_0 and R_L as spurious facet reflectivities to account for this effect.

We consider an active material with n_l QD layers and include in the analysis three confined states (the ground state GS and the two excited states ES_1, ES_2) and a quasi-2D state (wetting layer, WL). Occupation probabilities $\rho_i^l(z)$ in the confined states ($i = GS, ES_1, ES_2$) and for each layer l are calculated by solving a system of coupled rate equations [4] taking into account confined states filling, characteristic relaxation and escape times, non-radiative and Auger recombinations, stimulated and spontaneous emission. We assume that each QD layer receives a fraction $I(z)/n_l$ of the externally applied current $I(z)$, which depends on the longitudinal position, neglecting carrier transport effects.

The optical gain considers contribution from of all the confined states:

$$g_m(z) = \sum_{l=1}^{n_l} \sum_{i=GS,ES_1,ES_2} g_i G(E_m - E_i^l)(2\rho_i^l(z) - 1) \quad (2)$$

with g_i maximum gain of state i, $G(E)$ Gaussian distribution modeling the inhomogeneous broadening of the QD ensemble, E_i^l transition energies.

The differential equations for photons and carriers are integrated in space using a finite difference scheme; first, the distribution of carriers is calculated in absence of photons, and used as an initial guess for an iterative solver which updates the spatial distribution of photons and the filling of the QD states until convergence is reached.

III. Results

We validated the model results against the measurements performed on an SLD with 10 layers of InAs QDs organized in 3 groups of 3, 3 and 4 identical QD layers, with GS emission centered at 1211 nm, 1243 nm and 1285 nm, respectively [5]. The waveguide is formed by a first 500 μm long straight region, followed first by a 500 μm long tapered region (1.5° taper angle), and finally by a 5 mm long tapered region (0.8° taper angle). The waveguide widths at the rear (z=0) and front (z= 6 mm) facets are 14 μm and 110 μm, respectively. A shallow ridge is etched at the border of the waveguide to introduce a
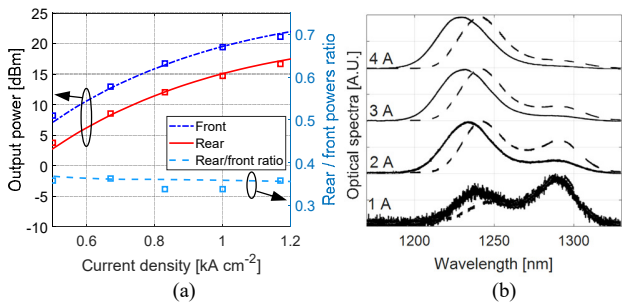
Fig.1. (a) Left axis: powers at the front (blue) and rear (red) facets; simulations (continuous line) and experiments (markers). Right axis: ratio of the rear and front facet powers; simulations (dashed line) and experiments (markers). (b) Experimental optical spectra at the front (continuous) and rear (dashed) facets for front facet currents from 1 A to 4 A with a fixed rear section current of 100 mA.

weak index guiding effect. Two electrodes are present, the rear one covering the straight waveguide, the first tapered waveguide and 875 µm of the second tapered waveguide, while the front one covers the remaining part of the second tapered waveguide, in such a way that the electrodes areas ratio is 1:5.5. Back reflections are minimized thanks to anti-reflection coatings applied to the end facets, and a 7° tilt of the waveguide relative to its facets. The device is operated at 20°C. Under uniform current injection, the device exhibits a strong asymmetry in the output optical power (Fig. 1a), with a maximum power at the front and rear facets of 120 mW and 47 mW, respectively. The maximum output power emitted from the front facet is 137.5 mW with injected currents of 0.7 A and 4 A at the rear and front electrodes, respectively; in this condition the rear facet output power is as high as 48.5 mW, with a total output power of 186.0 mW. Under non-uniform current injection, optical spectra at the two facets show an increasing asymmetry and a blue shift of the front facet spectra while increasing the front section current (Fig. 1b).

The normalized DOS used in the numerical simulations, associated to the 3 different QD layers, are shown in Fig. 2a, while example net gain curves resulting from the confined states filling is presented in Fig. 2b. We used the experimental data to fine tune the model parameters, reproducing the SLD light-current characteristic under uniform current injection (Fig.1a). Main parameters are 65% injection efficiency, 35 meV FWHM inhomogeneous broadening; the maximum gains for GS, ES_1 and ES_2 are 690 cm^{-1}, 750 cm^{-1}, 700 cm^{-1}, respectively; the capture time from ES_2 to ES_1 and from ES_1 to GS is 5 ps for all the layers. The model is able to correctly reproduce and explain the shift in the output spectra under a
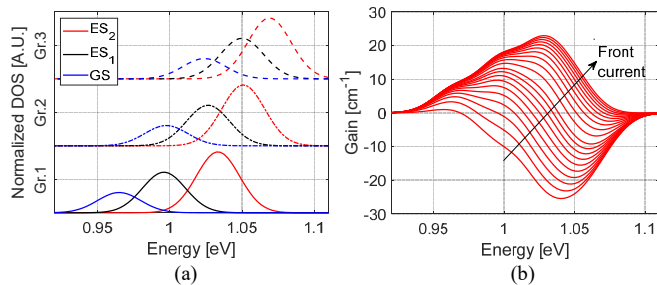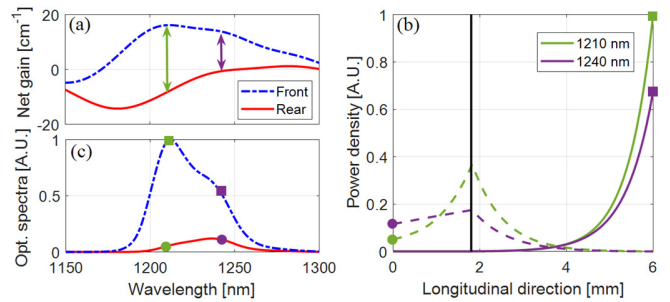

Fig.3. Simulations. (a) Net optical gain close to the front facet (dot-dashed blue line) and the rear facet (continuos line). Arrows indicate the net gain difference at 1210 nm and 1240 nm. (b) Longitudinal distribution of the photons at 1210 nm and 1240 nm propagating in the forward (continuous lines) and backward (dashed lines) directions. The vertical black line indicates the separation between the two electrodes. (c) Resulting optical spectra. Markers in (b) and (c) indicate the same points.

non-uniform current injection, as shown in detail in Fig. 3 for an exemplary case with a rear section current of 100 mA and a front section current of 3.5 A. Due to the strong non-uniform current injection, the occupation probabilities close to the two facets are sensibly different; in particular, the filling of ES_1 and ES_2 is much larger close to the front facet, while close to the rear facet only the ground states are above transparency. As a result, the net gain curves are significantly different. Photons with a wavelength of 1210 nm therefore experience a strong amplification in the front electrode, but are significantly absorbed in the rear section; on the other hand, photons at 1240 nm are amplified in the front section but are slightly absorbed in the rear one (Fig.3b). As a result, the spectrum at the rear facet presents a maximum at 1240 nm, while the spectrum at the front facet has a peak at 1210 nm (Fig. 3c).

CONCLUSIONS

We presented a model for the analysis and design of tapered multi-electrode SLDs, which can also be applied to weakly guided waveguides. The model can reproduce experimental findings and was applied to explain the strong reported asymmetry in the optical spectra of a chirped QD based SLD.

ACKNOWLEDGMENT

REFERENCES

[1] T. H. Ko et al., "Ultrahigh resolution optical coherence tomography imaging with a broadband superluminescent diode light source," Opt. Express 12, 2004, pp. 2112–2119.

[2] W. Denzer et al., "Near-infrared broad-band cavity enhanced absorption spectroscopy using a superluminescent light emitting diode," Analyst 134, 2009, pp. 2220–2223.

[3] P. Bardella at al., "Modeling of Broadband Chirped Quantum-Dot Super-Luminescent Diodes," IEEE J. Sel. Top. Quant. 15, 2009, pp. 785–791.

[4] A. F. Forrest et al., "Wide and tunable spectral asymmetry between narrow and wide facet outputs in a tapered quantum-dot superluminescent diode," Opt. Express 28, 2020, pp. 846–859.

[5] A. F. Forrest et al., "High-power quantum-dot superluminescent tapered diode under CW operation," Opt Express 27, 2019, pp. 10981–10990.

Fig.2. Simulations. (a) Normalized DOS in the three chirped QD layer for GS, ES_1 and ES_2. (b) Gain at the front facet for a 120 mA rear electrode current and a front electrode current uniformly varied from 160 mA to 5 A.